Supplementary Information

Site-specific glycosylation mapping of Fc gamma receptor IIIb from neutrophils of individual healthy donors.

Iwona Wojcik[1,2]*, Thomas Sénard[1]*, Erik L de Graaf[3], George MC Janssen[1], Arnoud H de Ru[1], Yassene Mohammed[1], Peter A van Veelen[1], Gestur Vidarsson[3], Manfred Wuhrer[1] and David Falck[1]

[1] Center for Proteomics and Metabolomics, Leiden University Medical Center, Leiden, The Netherlands
[2] Glycoscience Research Laboratory, Genos Ltd., Zagreb, Croatia
[3] Department of Experimental Immunohematology, Sanquin Research, and Landsteiner Laboratory, Academic Medical Center, University of Amsterdam, Amsterdam, The Netherlands
***Both authors contributed equally**

Correspondence and request for materials should be addressed to D.F. (email: d.falck@lumc.nl)

TABLE OF CONTENTS

ADDITIONAL EXPERIMENTAL DETAILS

Western blot:

At first, proteins were transferred from the gel onto a polyvinylidene difluoride (PVDF) membrane using an iBlot™2 Gel Transfer Device (ThermoFisher Scientific) at 20 V for 6 min. The membrane was then washed three times for 5 min with 1X Tris-Buffered Saline Tween 20 (TBST) and blocked with 5% milk (Elk, Campina, Amersfoort, The Netherlands) in TBST for 30 min. It was washed again thrice in TBST for 10 min before being incubated overnight at 4°C in 5% milk TBST with the anti-CD16 antibody diluted 1000 times. Thereafter, the membrane was washed three times for 10 min in TBST and then treated with enhanced chemiluminescent substrate (Pierce™ ECL Western Blotting Substrate, ThermoFisher Scientific). Both gels and western blots were visualized using a ChemiDoc MP Imaging system (Biorad, Hercules, USA), under Trans-UV for gels and chemiluminescence detection for membranes.

SUPPLEMENTARY FIGURES AND TABLES

Table S1. Information on healthy donors and separated neutrophils cells used for FcγRIIIb isolation.

Donor information	Donor 1	Donor 2	Donor 3
Sex	female	male	female
Cell type	neutrophils	neutrophils	neutrophils
Cell count [cell/mL]	$50x10^6$	$50x10^6$	$50x10^6$
Total protein con. [mg/mL]	1.61	1.72	1.51
Amount of cells for isolation [cell/mL]	$16x10^6$	$15x10^6$	$17x10^6$
Volume of lysate for isolation [µL]	310	291	331
Amount of total protein for isolation [µg]	500	500	500

Table S3. The search parameters used for initial analysis using Byonic (Protein Metrics, Cupertino, CA v3.2-38).

Search parameter	Value
Protein database	UniProt human protein database
Glycan database	User defined, see Table S2
Mass accuracy of precursor ions	5 ppm
Fragmentation type	QTOF/HCD
Parent tolerance	0.005 *m/z*
Mass accuracy of fragment ions	20 ppm
Recalibration (lock mass)	none
Maximum precursor mass	10,000
Precursor and mass charge assignments	compute from MS1
Max # of precursor per scan	2
Smoothing width	0.01 *m/z*

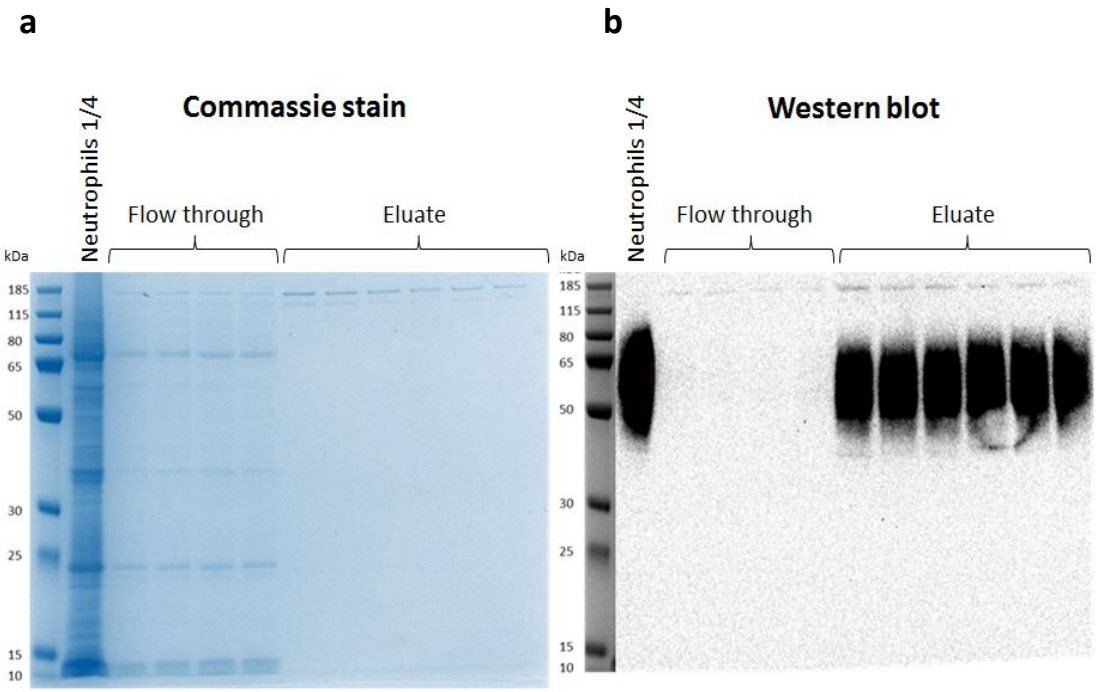

Figure S1. The whole non-reducing SDS-PAGE and western blot of human neutrophil lysate before and after FcγRIII immunoprecipitation. Protein contaminations and FcγRIIIb were detected with (a) commassie staining and (b) western blot, respectively. The neutrophils lanes represent ~25 µg of total protein content from the neutrophil cell lysate from donor 2. In this experiment, the immunoprecipitation was done from 100 µg and the eluate was split between the two gels (50 µg per gel). The flow-through lanes show the unbound diluted fraction of the immunoprecipitation while the eluate lanes present the purified FcγRIIIb protein. As expected, FcγRIIIb exhibits an elongated band from 50 to 80 kDa, visible after western blotting. Despite high dilution, the flow-through mirrors the major bands from the total cell lysate. In contrast, the eluate exhibits none of those bands and thus any interfering proteins of 50-80 kDa above the limit of detection (LOD; 25 ng protein). Two bands around 150 kDa appear in the flow-through and eluate. They are likely derived from the capturing antibody, as an in-solution proteolytic cleavage of the eluate revealed immunoglobulin G glycopeptide masses (data not shown). Whatever the identity of the contamination, it is the main reason to prefer an in-gel proteolytic cleavage.

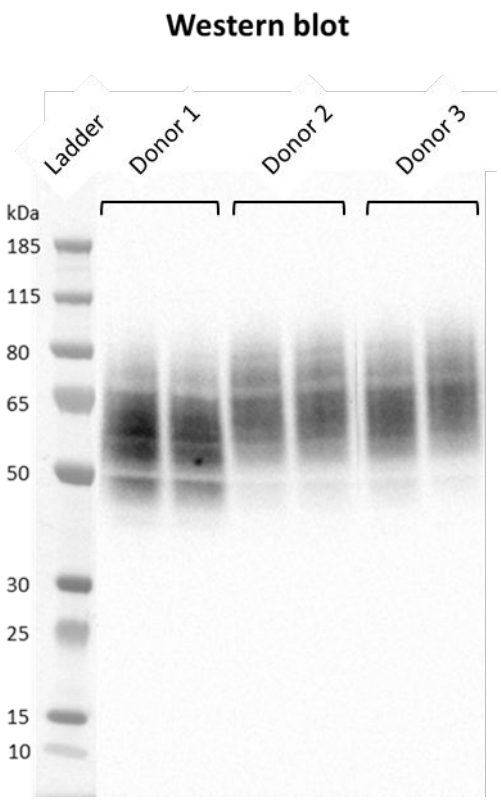

Figure S2. The immunoblot shows FcγRIIIb immunoprecipitated from the lysate of neutrophils. Lanes contain material from donor 1 (NA1/NA2), donor 2 (NA2/NA2) and donor 3 (NA2/NA2) in duplicate. Size markers are indicated on the left. FcγRIIIb showed a smear from 50 to 80 kDa indicating the heterogeneity of the *N*-glycosylation pattern of the receptor. Differential electrophoretic mobility of the receptor from NA1/NA2-heterozygous and NA2-homozygous is likely mainly due to NA polymorphism and distinct number of N-glycosylation sites[1]. Larger proteoforms attributed to NA2, may not be visible in the first donor, because the protein expression is skewed towards NA1.

Table S5. Byonic output of critical parameters reflecting the quality of the peptide-spectrum matches (PSMs) of identified FcyRIIIb for each donor. The list of parameters includes: protein p-value (the likelihood of the PSMs to be the identified protein). # unique peptides (total number of PSMs). coverage % (percent of the protein sequence covered by PSMs).

Donor	Protein Identified	Protein p-value (Log base 10)	# unique peptides	Ranking place	Coverage
1	Low affinity immunoglobulin gamma Fc region receptor III-B UNIPROT: O75015 (FCG3B_HUMAN)	362.01	131	1	77.8 %
2		268.28	127	1	80.3 %
3		250.22	114	1	71.2 %

Table S6. Characterization of predominant human FcγRIIIb (UniProtKB - O75015) site-specific peptides and glycopeptides generated from Endoproteinase Glu-C and chymotrypsin cleavage. C, carboxymethyl cysteine

Site	Peptide sequence	Glycosylation	*m/z* peptide [M+H]	*m/z* peptide [M+GlcNAc]	RT [min]
Asn 38	missing peptide	NA	NA	NA	NA
Asn 45	FHN(45)ES(47)LISSQASSY	+	1569.708	1772.787	17 - 23
Asn 64	FIDAATVN(64)DSGEY	-	1401.617	1604.696	19
Asn 74	RCQTN(74)LSTLSDPVQLE	+	1860.901	2063.980	20-28
	RCQTN(74)LSTLSDPVQLE	-	1860.901	-	25
Asn 162	CRGLVGSKN(162)VSSE	+	1392.679	1595.758	10 - 14
Asn 169	TVN(169)ITITQGLAV	+	1229.706	1432.779	28 - 32

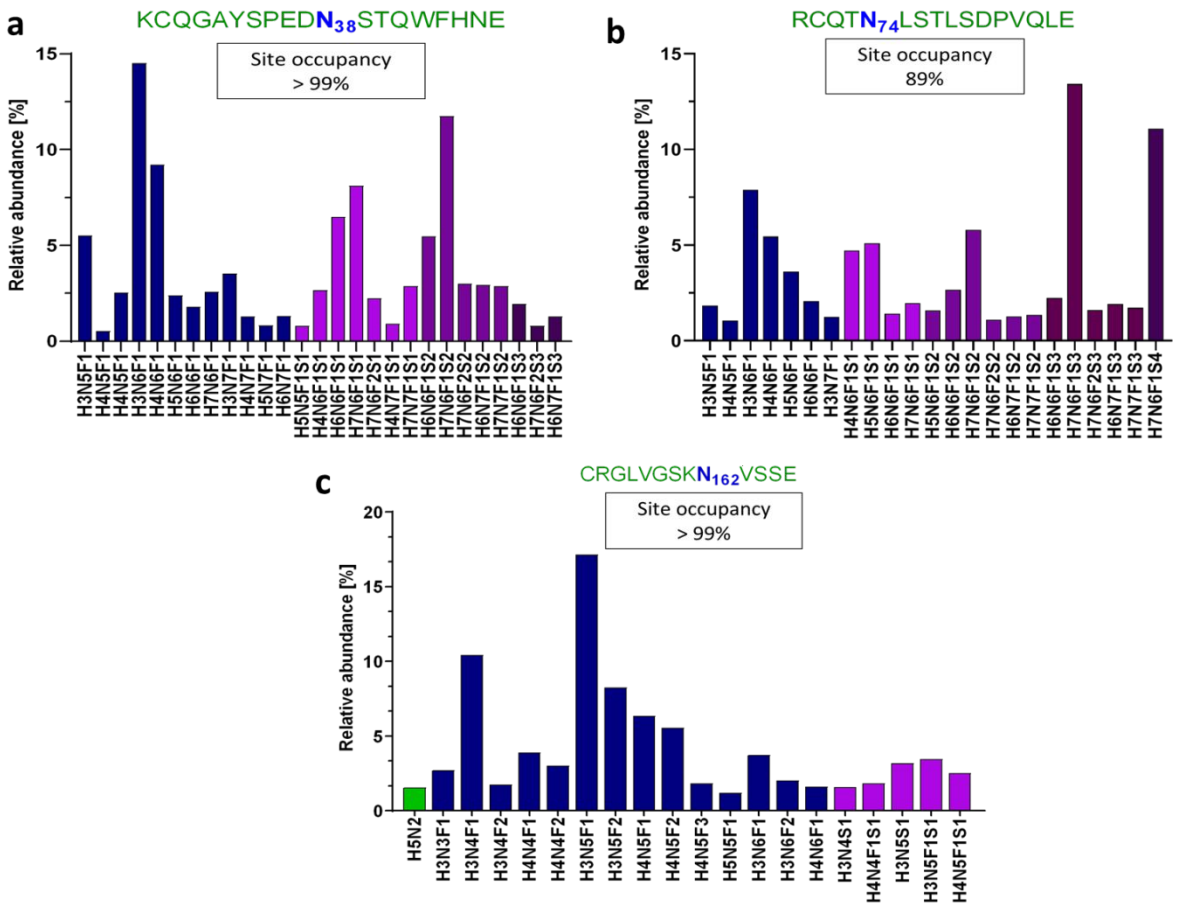

Figure S3. Bar graphs showing the relative abundances of identified glycopeptides for recombinant NA1 allotype of FcγRIIIb[2]. Site-specific analysis revealed (a) 27 different glycan compositions occupying the glycosylation site N_{38}, (b) 54 compositions on site N_{74} and (c) 65 compositions on site N_{162}. For sites N_{74} and N_{162} only compositions above a 1% cut-off of relative abundance were visualized, amounting to 23 and 20 glycans respectively. Full glycosylation site occupancy was observed for N_{38} and N_{162}, while site N_{74} was partially occupied. 11% relative signal intensity of the non-glycosylated peptide were detected. Sulphated and multifucosylated *N*-glycan compositions were detected below 1% relative intensity for N_{74}, as were sulphated and disialylated *N*-glycans for N_{162}. Bar colours indicate glycan classes: Green, oligomannose type; blue, neutral complex; purple, sialylated complex, with one (light), two (medium) or three (dark) sialic acids per glycan.

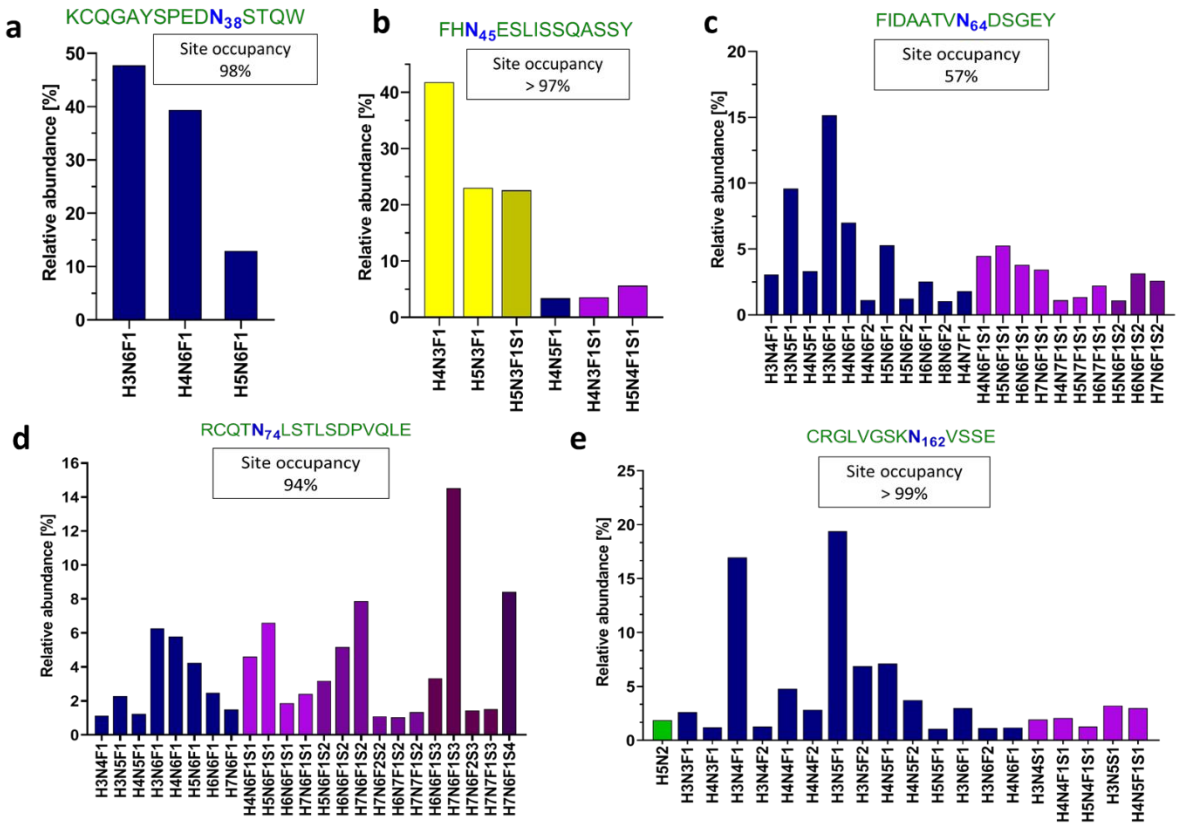

Figure S4. Bar graphs showing the relative abundances of identified glycopeptides for the recombinant NA2 allotype of FcγRIIIb[2]. Site-specific analysis revealed (a) 3 different glycan compositions occupying the glycosylation site N_{38}, (b) 6 compositions on site N_{45}, (c) 35 compositions on site N_{64}, (d) 49 compositions on site N_{74} and (e) 69 compositions on site N_{162}. For sites N_{64}, N_{74} and N_{162} only compositions above a 1% cut-off of relative abundance were visualized, amounting to 21, 23 and 20 glycans respectively. Full glycosylation site occupancy was observed for N_{45} and N_{162}, while sites N_{38}, N_{64} and N_{74} were partially occupied. 2%, 46% and 7% relative signal intensity of the non-glycosylated peptide for sites N_{38}, N_{64} and N_{74} were detected respectively. Multifucosylated *N*-glycan compositions for N_{64}, sulfated *N*-glycans for N_{74} and sulphated and disialylated *N*-glycans for N_{162} were detected below 1% relative intensity. Bar colours indicate glycan classes: Yellow, hybrid, sialylated hybrid (medium); Green, oligomannose type; blue, neutral complex; purple, sialylated complex, with one (light), two (medium) or three (dark) sialic acids per glycan.

Table S7. Allelic peptide and glycopeptide sequences containing N45 and N64/D64 used for polymorphic variant assessment. *Uniprot identifiers.

FcyRIII variant	N_{45} peptide		N_{64} peptide
NA1 *O75015 (FCG3B*01)	FHN$_{45}$EN(47)LISSQASSY		FIDAATVD$_{64}$DSGEY
NA2 *O75015 (FCG3B*02)	FH**N**$_{45}$ES(47)LISSQASSY		FIDAATV**N**$_{64}$DSGEY
FcyRIIIa *P08637	FH**N**$_{45}$ES(47)LISSQASSY		FIDAATVD$_{64}$DSGEY
DONOR	RATIO ALLOTYPIC		ALLOTYPE
	NES/(NES+NEN)	NDS/(DDS+NDS)	
Donor 1	0.2	0.26	NA1/NA2
Donor 2	0.99	0.98	NA2/NA2
Donor 3	0.99	0.98	NA2/NA2

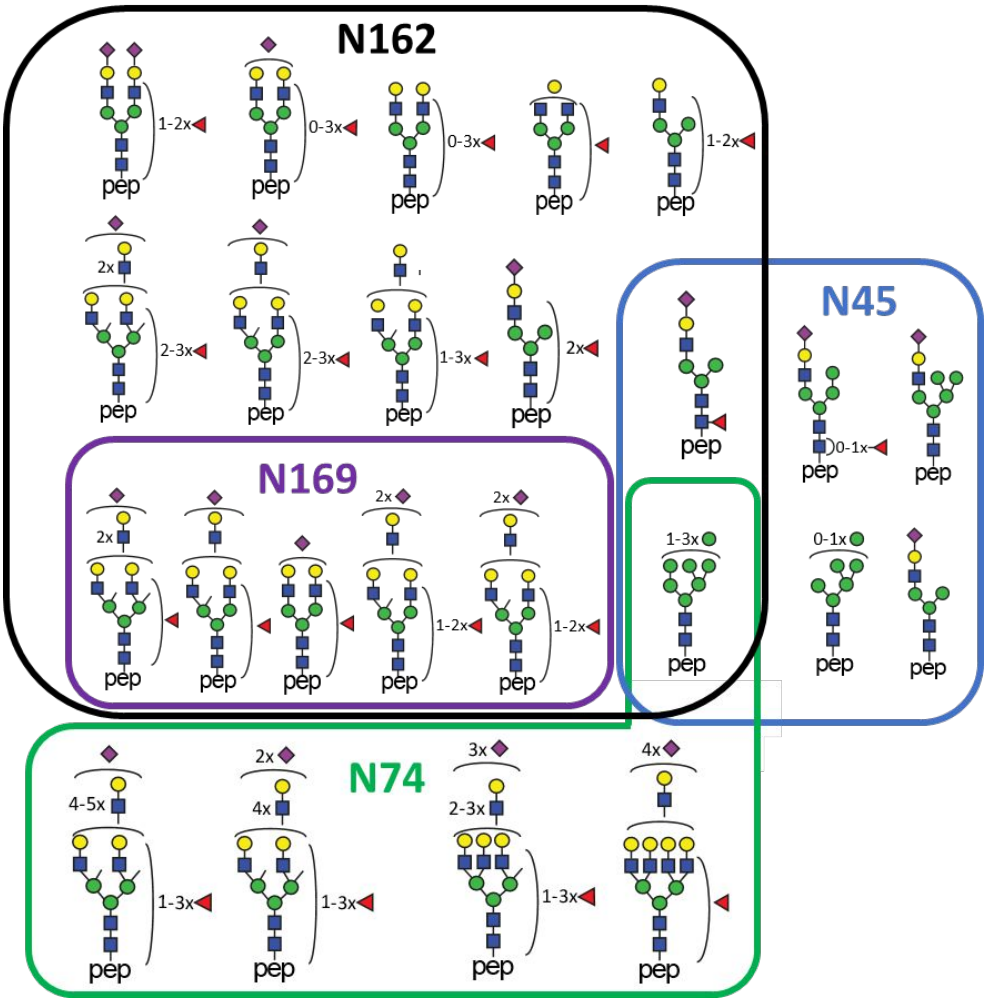

Figure S5. Putative structures of N-glycans identified on the four occupied *N*-glycosylation sites, namely 10 at N_{45}, 15 at N_{74}, 30 at N_{162} and 6 at N_{169}. Isomeric structures co-occur and are discussed in the text. The scheme underlines the diversity, overlap and uniqueness of glycans compositions.

Table S8. The glycosylation profiles of endogenous neutrophil-derived FcyRIIIb, soluble FcyRIIIb and NK-derived FcyRIIIa. The different glycoforms are displayed as defined derived traits (high mannose, complex, hybrid). *the corresponding glycopeptides were not detected in this study **potential glycosylation site was not occupied by oligosaccharides, only corresponding peptide observed.

Sites	FcyRIIIb – our study (human neutrophils)	sFcyRIIIb[3] (human serum)	FcyRIIIb[4] (human neutrophils)	FcyRIIIa[5] (human natural killer cells)
N_{38}	-*	Complex (LacNAc repeats) > 99%	- *	Complex (LacNAc repeats) > 99%
N_{45}	Complex (monoantennary) 8% Hybrid 7% High mannose 86%	High mannose >99%	Complex (monoantennary) 16% Hybrid < 30% High mannose 54%	Complex (di-, tri-, tetra antennary) 22% Hybrid 71% High mannose 2%
N_{64}	-** (not glycosylated)	Complex (LacNAc repeats) > 99%	- ** (not glycosylated)	-
N_{74}	Complex (LacNAc repeats) 86% High mannose 14%	Complex (LacNAc repeats) > 99 %	- *	Complex (LacNAc repeats) > 99%
N_{162}	Complex (mono-, di- , tri antennary) 98% High mannose 2%	Complex (di-, tri-, tetraantennary) > 99%	Complex (di-, tri antennary) > 99%	Complex (di-, tri-antennary) 66% Hybrid 22% High mannose 12%
N_{169}	Complex (di-, tri-, tetrantennary) > 99%	Complex (di-, tri-, tetrantennary) > 99%	- *	Complex (di-, tri-, tetrantennary) > 99%

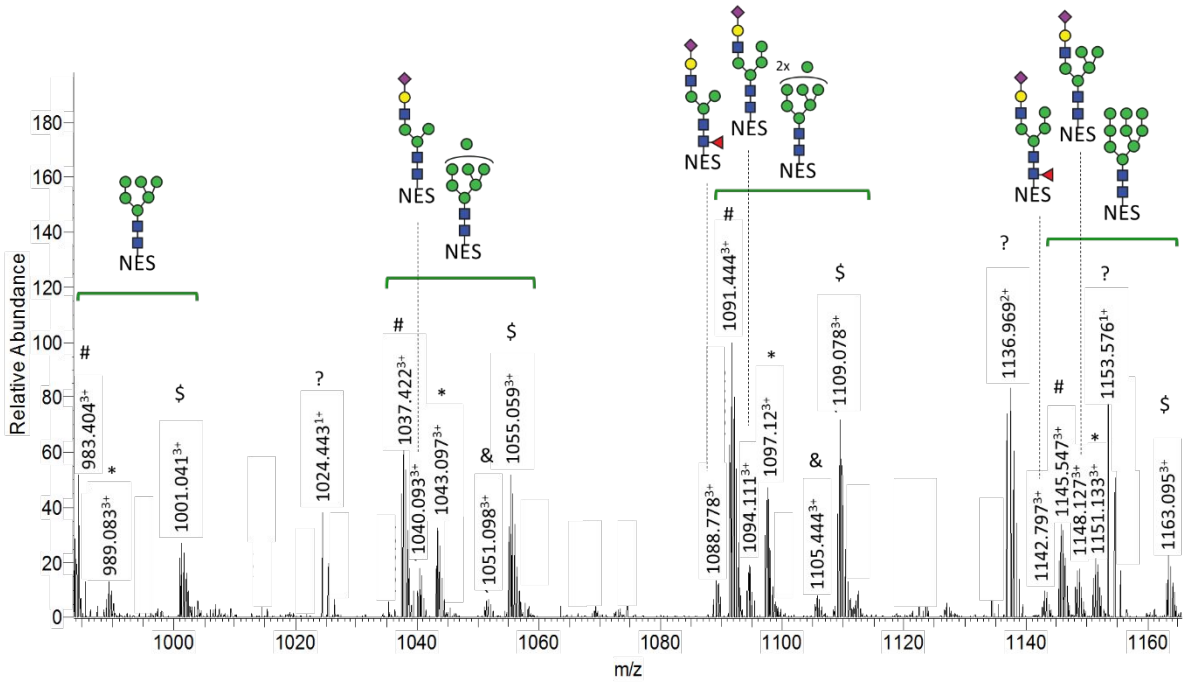

Figure S6. Sum spectra showing the different ions observed for the N_{45} glycoforms of FcγRIIIb. The mass spectrum was generated for donor 2 within the following retention time range: 17.4-19.4 min. NES: FH**N_{45}**ESLISSQASSY peptide backbone. The MS spectra revealed satellite peaks for some triply-charged protonated species with a difference of 55.934 Da and 18.033 Da. These were identified by accurate mass (< ± 5 ppm) as iron ($[M+Fe^{III}]^{3+}$) and ammonia ($[M+2H+NH_4]^{3+}$) adducts, respectively. They also presented the same retention time as the respective protonated glycopeptide. Additionally, the presence of the ammonia adducts was confirmed by MS/MS spectra, as the comparison of the b- and y-ion series provided evidence for the same peptide backbone without additional modification. #: the triply protonated N_{45} glycopeptides $[M+3H]^{3+}$. *: the triply charged ions of protonated N_{45} glycopeptides with ammonia adducts $[M+2H+NH_4]^{3+}$. $: N_{45} glycopeptides charged by iron ions $[M+Fe^{III}]^{3+}$. &: misscleaved glycopeptide. ?: unidentified glycopeptide.

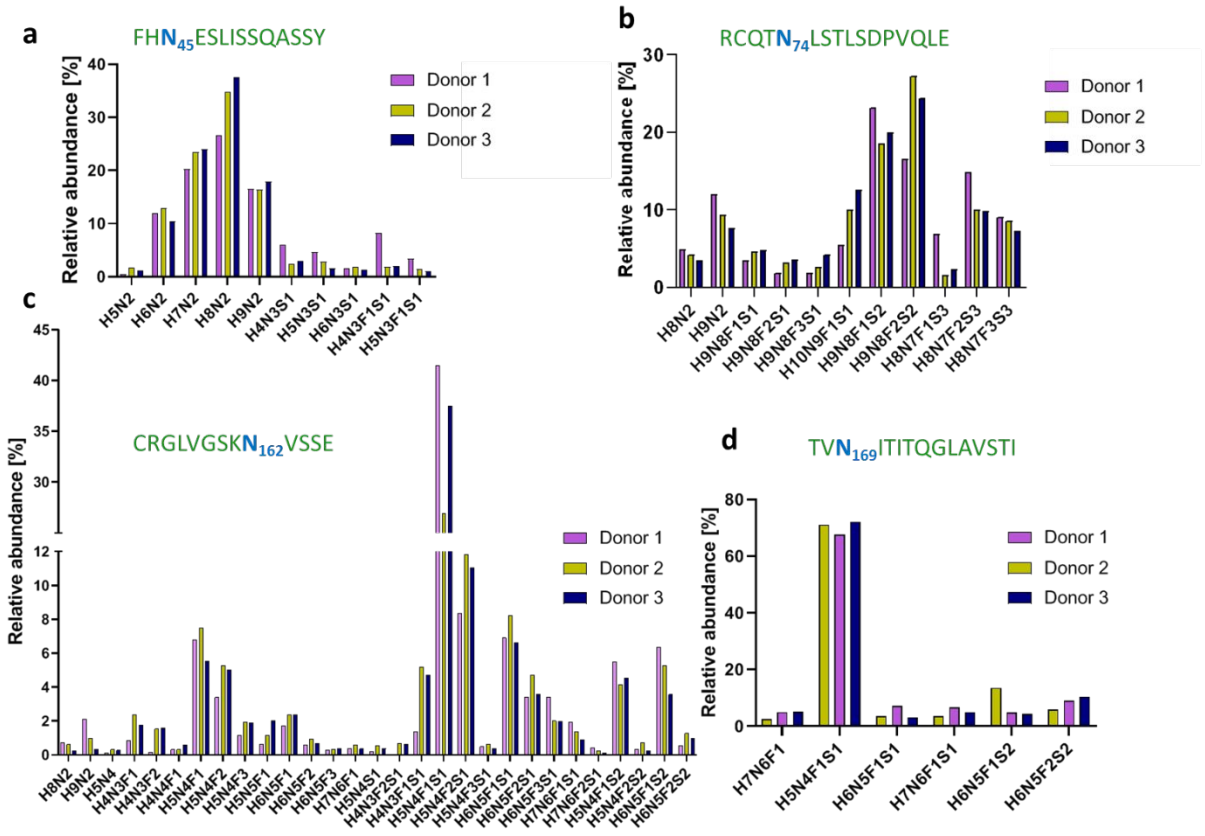

Figure S7. Site-specific relative quantification of FcγRIIIb glycoforms. Bar graphs show the relative abundance of identified glycopeptides for individual donors, donor 1 (NA1/NA2), donor 2 (NA2/NA2) and donor 3 (NA2/NA2). (a) 10 different glycan compositions occupy glycosylation site N_{45}, (b) 11 site N_{74}, (c) 30 site N_{162} and (d) 6 site N_{169}.

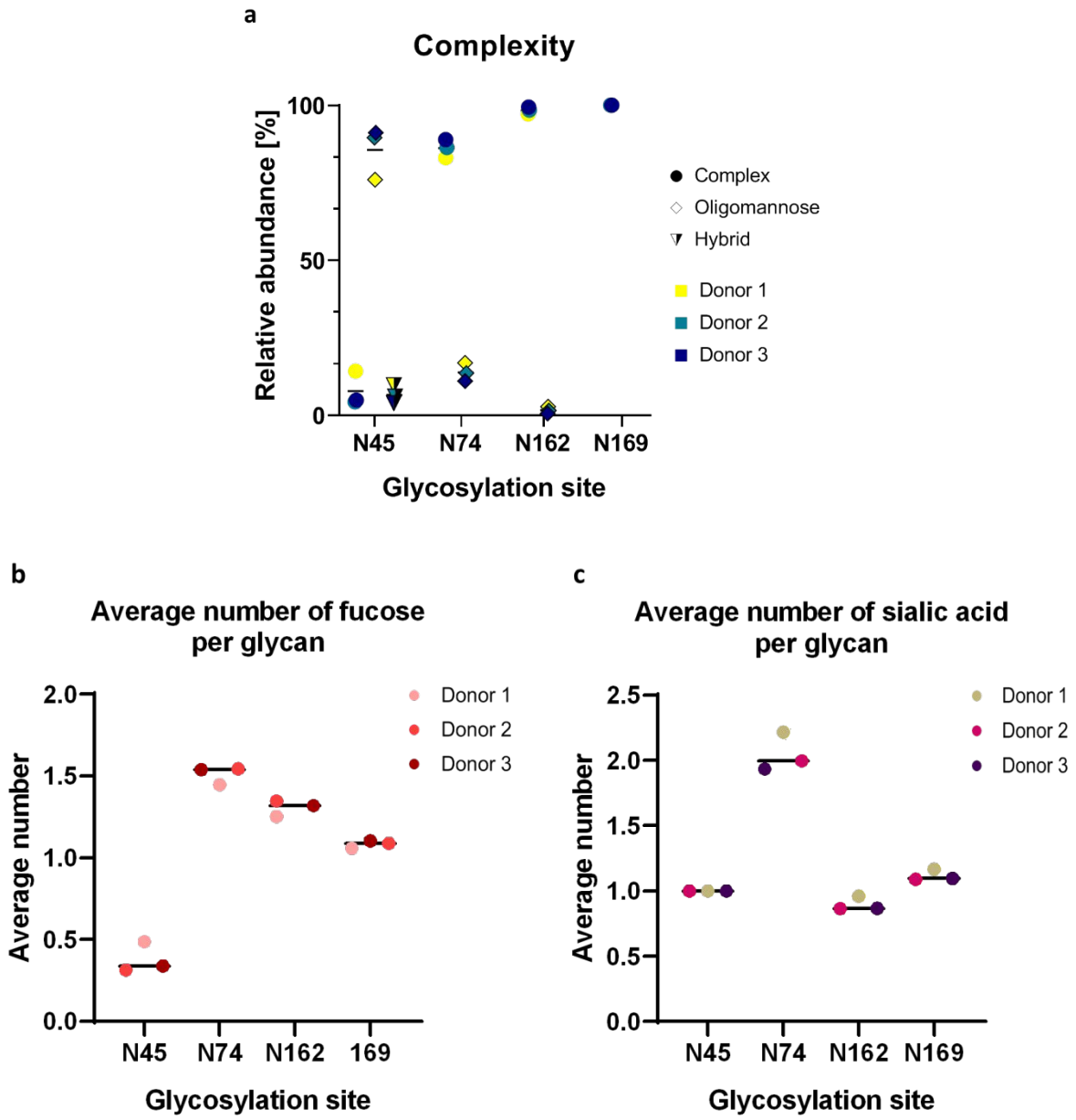

Figure S8. Various glycosylation parameters were calculated to evaluate the glycosylation profile of FcγRIIIb. Displayed is the average and standard deviation per glycosylation site of the three donors, donor 1 (NA1/NA2), donor 2 (NA2/NA2) and donor 3 (NA2/NA2), regarding several derived glycosylation traits: (a) the relative abundance of the three basic N-glycans types; (b) the average number of fucoses per glycan; (c) the average number of sialic acids per glycan. For detailed calculation of the presented traits refer to **Table S10**.

Table S9. Site-specific derived glycosylation traits. Average number of sialic acids and fucoses per glycan of endogenous neutrophil-derived FcγRIIIb, soluble FcγRIIIb and NK-derived FcγRIIIa. *the corresponding glycopeptides were not detected in this study **potential glycosylation site was not occupied by oligosaccharides, only corresponding peptide observed. For detailed calculations of the traits, see **Table S10**.

Sites	Derived traits	FcγRIIIb – our study	sFcγRIIIb[3] (human serum)	FcγRIIIb[4] (human neutrophils)	FcγRIIIa[5] (human NK cells)
N_{38}	average number of sialic acids	-*	3.3	- *	4.0
	average number of fucoses		2.2		1.0
N_{64}	average number of sialic acids	-**	2.5	- **	-
	average number of fucoses		1.3		
N_{45}	average number of sialic acids	1.0	0.0	1.0	1.2
	average number of fucoses	0.5	0.0	0.5	0.5
N_{74}	average number of sialic acids	2.1	3.7	- *	4.0
	average number of fucoses	1.5	2.0		1.1
N_{162}	average number of sialic acids	0.9	1.1	1.1	1.3
	average number of fucoses	1.3	1.2	1.2	1.1
N_{169}	average number of sialic acids	1.1	1.5	- *	1.5
	average number of fucoses	1.1	1.2		1.0

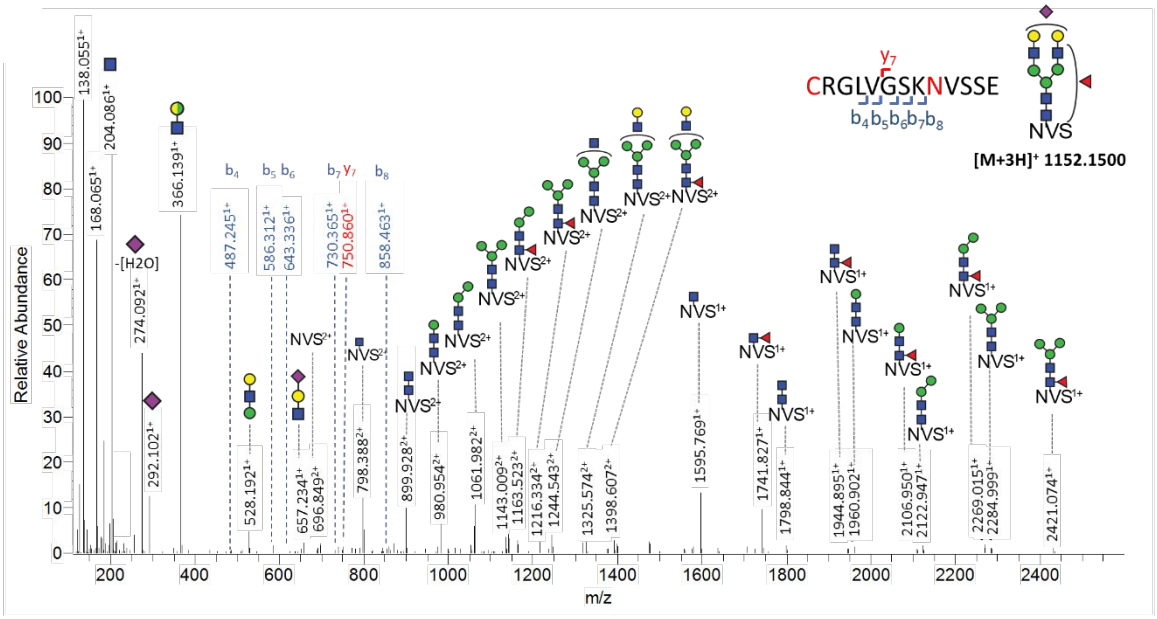

Figure S9. Stepping-energy HCD MS/MS sum spectrum of the precursor ion 1152.150^{3+} [second isotopologue] of the most abundant N_{162} glycopeptide (H5N4F1S1). The MS/MS spectrum was generated for three stepping energies (32%, 37%, 42% NCE) at retention time 11.0 min.

Table S10. Site-specific derived trait calculation. The compositions are placeholders for their respective relative intensities.

Site	NUMBER OF SIALIC ACIDS Average number of sialic acids per glycan on complex glycans of FcγRIIIb
N_{45}	(H4N3S1 + H4N3F1S1) / (H4N3S1 + H4N3F1S1)
N_{74}	(H9N8F1S1 + H9N8F2S1 + H9N8F3S1 + H10N9F1S1) + 2*(H9N8F1S2 +H9N8F2S2) + 3*(H8N7F1S3+H8N7F2S3+H8N7F3S3)) / (H9N8F1S1 + H9N8F2S1 + H9N8F3S1 + H10N9F1S1 + H9N8F1S2 + H9N8F2S2 + H8N7F1S3 + H8N7F2S3 + H8N7F3S3)
N_{162}	(H5N4S1 + H4N3F2S1 + H4N3F1S1 + H5N4F1S1 + H5N4F2S1 + H5N4F3S1 + H6N5F1S1 + H6N5F2S1 + H6N5F3S1 + H7N6F1S1 + H7N6F2S1) + 2*(H5N4F1S2 + H5N4F2S2 + H6N5F1S2 + H6N5F2S2)) / (H5N4 + H4N3F1 + H4N3F2 + H4N4F1 + H5N4F1 + H5N4F2 + H5N4F3 + H5N5F1 + H6N5F1 + H6N5F2 + H6N5F3 + H7N6F1 + H5N4S1 + H4N3F2S1 + H4N3F1S1 + H5N4F1S1 + H5N4F2S1 + H5N4F3S1 + H6N5F1S1 + H6N5F2S1 + H6N5F3S1 + H7N6F1S1 + H7N6F2S1 + H5N4F1S2 + H5N4F2S2 + H6N5F1S2 + H6N5F2S2)
N_{169}	(H5N4F1S1 + H6N5F1S1 + 2*(H6N5F1S2 + H6N5F2S2) + H7N6F1S1) / (H5N4F1S1 + H6N5F1S1 + H6N5F1S2 + H6N5F2S2 + H7N6F1S1 + H7N6F1)
Site	NUMBER OF FUCOSES Average number of fucoses per glycan on complex glycans of FcγRIIIb
N_{45}	(H4N3F1S1) / (H4N3S1 + H4N3F1S1)
N_{74}	(H9N8F1S1 + H10N9F1S1 + H9N8F1S2 + H8N7F1S3) + 2*(H9N8F2S1 + H9N8F2S2+H8N7F2S3) + 3*(H9N8F3S1+H8N7F3S3) / (H9N8F1S1 + H9N8F2S1 + H9N8F3S1 + H10N9F1S1 + H9N8F1S2 + H9N8F2S2 + H8N7F1S3 + H8N7F2S3 + H8N7F3S3)
N_{162}	(H4N3F1 + H4N4F1 + H5N4F1 + H5N5F1 + H6N5F1 + H7N6F1 + H4N3F1S1 + H5N4F1S1 + H6N5F1S1 + H7N6F1S1 + H5N4F1S2 + H6N5F1S2 + 2*(H4N3F2 + H5N4F2 + H6N5F2 + H4N3F2S1 + H5N4F2S1 + H6N5F2S1 + H7N6F2S1 + H5N4F2S2 + H6N5F2S2) + 3*(H5N4F3 + H6N5F3 + H5N3F3S1 + H6N5F3S1) / (H5N4 + H4N3F1 + H4N3F2 + H4N4F1 + H5N4F1 + H5N4F2 + H5N4F3 + H5N5F1 + H6N5F1 + H6N5F2 + H6N5F3 + H7N6F1 + H5N4S1 + H4N3F2S1 + H4N3F1S1 + H5N4F1S1 + H5N4F2S1 + H5N4F3S1 + H6N5F1S1 + H6N5F2S1 + H6N5F3S1 + H7N6F1S1 + H7N6F2S1 + H5N4F1S2 + H5N4F2S2 + H6N5F1S2 + H6N5F2S2)
N_{169}	(H7N6F1 + H7N6F1S1 + H5N4F1S1 + H6N5F1S1 + H6N5F1S2 + 2*H6N5F2S2) / (H5N4F1S1 + H6N5F1S1 + H6N5F1S2 + H6N5F2S2 + H7N6F1S1 + H7N6F1)
Site	HIGH MANNOSE Fraction of high mannose glycans
N_{45}	(H5N2 + H6N2 + H7N2 + H8N2 + H9N2) / (H5N2 + H6N2 + H7N2 + H8N2 + H9N2 + H4N3S1 + H5N3S1 + H6N3S1 + H4N3F1S1 + H5N3F1S1)
N_{74}	(H8N2 + H9N2) / (H8N2 + H9N2 + H9N8F1S1 + H9N8F2S1 + H9N8F3S1 + H10N9F1S1 + H9N8F1S2 + H9N8F2S2 + H8N7F1S3 + H8N7F2S3 + H8N7F3S3)
N_{162}	(H8N2 + H9N2) / (H8N2 + H9N2 + H5N4 + H4N3F1 + H4N3F2 + H4N4F1 + H5N4F1 + H5N4F2 + H5N4F3 + H5N5F1 + H6N5F1 + H6N5F2 + H6N5F3 + H7N6F1 + H5N4S1 + H4N3F2S1 + H4N3F1S1 + H5N4F1S1 + H5N4F2S1 + H5N4F3S1 + H6N5F1S1 + H6N5F2S1 + H6N5F3S1 + H7N6F1S1 + H7N6F2S1 + H5N4F1S2 + H5N4F2S2 + H6N5F1S2 + H6N5F2S2)
N_{169}	-
Site	HYBRID Fraction of hybrid glycans
N_{45}	(H5N3S1 + H6N3S1 + H5N3F1S1) / (H5N2 + H6N2 + H7N2 + H8N2 + H9N2 + H4N3S1 + H5N3S1 + H6N3S1 + H4N3F1S1 + H5N3F1S1)
N_{74}	-
N_{162}	-
N_{169}	-
Site	COMPLEX Fraction of complex glycans
N_{45}	(H4N3S1 + H4N3F1S1) / (H5N2 + H6N2 + H7N2 + H8N2 + H9N2 + H4N3S1 + H5N3S1 + H6N3S1 + H4N3F1S1 + H5N3F1S1)
N_{74}	(H9N8F1S1 + H9N8F2S1 + H9N8F3S1 + H10N9F1S1 + H9N8F1S2 + H9N8F2S2 + H8N7F1S3 + H8N7F2S3 + H8N7F3S3) / (H8N2 + H9N2 + H9N8F1S1 + H9N8F2S1 + H9N8F3S1 + H10N9F1S1 + H9N8F1S2 + H9N8F2S2 + H8N7F1S3 + H8N7F2S3 + H8N7F3S3)
N_{162}	(H5N4 + H4N3F1 + H4N3F2 + H4N4F1 + H5N4F1 + H5N4F2 + H5N4F3 + H5N5F1 + H6N5F1 + H6N5F2 + H6N5F3 + H7N6F1 + H5N4S1 + H4N3F2S1 + H4N3F1S1 + H5N4F1S1 + H5N4F2S1 + H5N4F3S1 + H6N5F1S1 + H6N5F2S1 + H6N5F3S1 + H7N6F1S1 + H7N6F2S1 + H5N4F1S2 + H5N4F2S2 + H6N5F1S2 + H6N5F2S2) / (H8N2 + H9N2 + H5N4 + H4N3F1 + H4N3F2 + H4N4F1 + H5N4F1 + H5N4F2 + H5N4F3 + H5N5F1 + H6N5F1 + H6N5F2 + H6N5F3 + H7N6F1 + H5N4S1 + H4N3F2S1 + H4N3F1S1 + H5N4F1S1 + H5N4F2S1 + H5N4F3S1 + H6N5F1S1 + H6N5F2S1 + H6N5F3S1 + H7N6F1S1 + H7N6F2S1 + H5N4F1S2 + H5N4F2S2 + H6N5F1S2 + H6N5F2S2)
N_{169}	(H7N6F1 + H5N4F1S1 + H6N5F1S1 + H7N6F1S1 + H6N5F1S2 + H6N5F2S2) / (H7N6F1 + H5N4F1S1 + H6N5F1S1 + H7N6F1S1 + H6N5F1S2 + H6N5F2S2)

References

(1) Huizinga, T. W.; de Haas, M.; Kleijer, M.; Nuijens, J. H.; Roos, D.; von dem Borne, A. E. *J Clin Invest* **1990**, *86*, 416-423.
(2) Dekkers, G.; Treffers, L.; Plomp, R.; Bentlage, A. E. H.; de Boer, M.; Koeleman, C. A. M.; Lissenberg-Thunnissen, S. N.; Visser, R.; Brouwer, M.; Mok, J. Y.; Matlung, H.; van den Berg, T. K.; van Esch, W. J. E.; Kuijpers, T. W.; Wouters, D.; Rispens, T.; Wuhrer, M.; Vidarsson, G. *Front Immunol* **2017**, *8*, 877.
(3) Yagi, H.; Takakura, D.; Roumenina, L. T.; Fridman, W. H.; Sautes-Fridman, C.; Kawasaki, N.; Kato, K. *Sci Rep* **2018**, *8*, 2719.
(4) Washburn, N.; Meccariello, R.; Duffner, J.; Getchell, K.; Holte, K.; Prod'homme, T.; Srinivasan, K.; Prenovitz, R.; Lansing, J.; Capila, I.; Kaundinya, G.; Manning, A. M.; Bosques, C. J. *Mol Cell Proteomics* **2019**, *18*, 534-545.
(5) Patel, K. R.; Nott, J. D.; Barb, A. W. *Mol Cell Proteomics* **2019**, *18*, 2178-2190.